

Supplementary Information

**Polarons in single-layer MnBr₂: properties and dependence on
the substrate**

Affan Safeer,^{1,*} Oktay Güleryüz,¹ Guangyao Miao,¹
Wouter Jolie,¹ Thomas Michely,¹ and Jeison Fischer¹

¹*II. Physikalisches Institut, Universität zu Köln,*

Zülpicher Straße 77, 50937 Köln, Germany

* safeer@ph2.uni-koeln.de

CONTENTS

Supplementary note 1: Extended dataset for bias-dependent polaron imaging and mobility.	3
Supplementary note 2: Mobility of type-I mobile polaron for lower positive V_b at large tunneling current	5
Supplementary Note 3: Overview topographs of single-layer MnBr ₂ grown on different substrates.	6
Supplementary note 4: Polarons in MnBr ₂ on Gr/Ir(111)	7
Supplementary note 5: Tip induced conversions of type-II 1x1 polarons into type-I mobile polarons.	8
Supplementary note 6: Creation of a type-I 1x1 mobile polaron in MnBr ₂ on Gr/Ir(111).	9
Supplementary note 7: Bias dependent absolute tip heights above Gr/Ir(110) and MnBr ₂ /Gr/Ir(110).	10

Supplementary note 1: Extended dataset for bias-dependent polaron imaging and mobility.

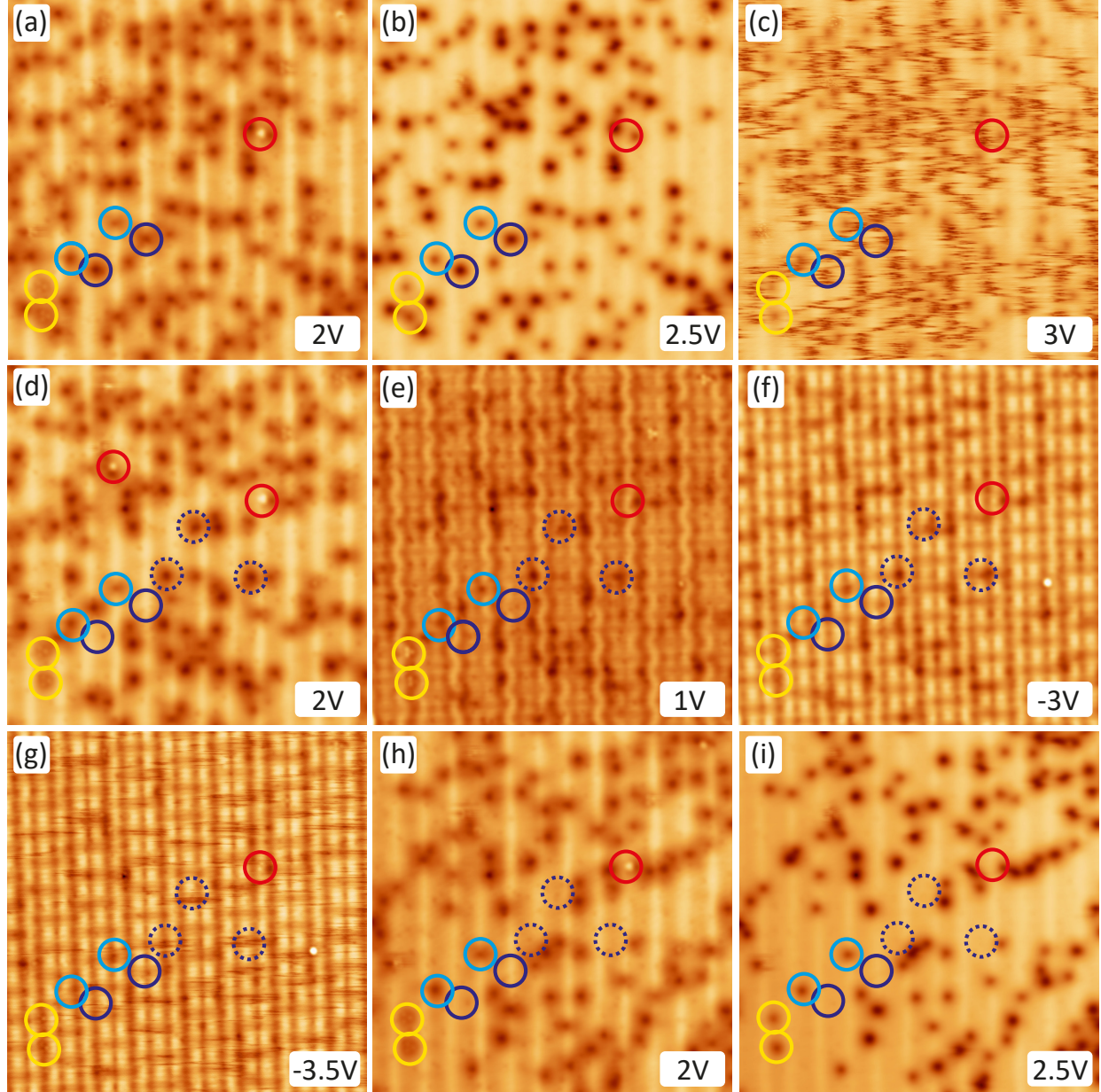


Figure S1. (a-i) Sequence of STM images of the same area acquired at varying V_b ranging from $+3\text{ V}$ and -3.5 V , as indicated, and at $I_t = 50\text{ pA}$. Selected polarons are encircled to track their position: dark blue (type-I mobile), light blue (type-I immobile), yellow (type-II 2x2), and red (type-II 1x1). From comparison of (d) and (h) it is obvious that type-I mobile polarons are also moved at $V_b = -3.5\text{ V}$. Image sizes: $45\text{ nm} \times 45\text{ nm}$.

Figure S1 presents a complementary dataset to Figure 2 of the main text, extending the investigation to higher negative bias range. The behavior at positive V_b [Figure S1(a-e)] is consistent with our previous observations. The four types of polarons are distinguishable at $V_b = 2$ V, and type-I mobile polarons change positions after increasing V_b to 3 V, as tracked by the polarons encircled dark blue in Figure S1(a-d).

The tip-induced mobility is also observed at negative V_b . If V_b is set to -3.5 V in Figure S1(g), type-I mobile polarons are mobile as obvious from the comparison of Figures S1(d) and (h) (check position in dotted dark blue circles).

Supplementary note 2: Mobility of type-I mobile polaron for lower positive V_b at large tunneling current

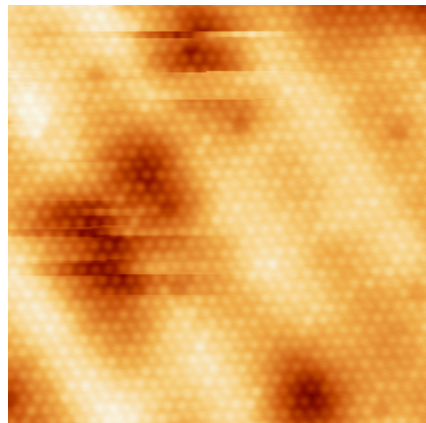


Figure S2. STM image acquired with $V_b = 2$ V, $I_t = 3$ nA. Image size: 15 nm \times 15 nm.

Supplementary Note 3: Overview topographs of single-layer MnBr₂ grown on different substrates.

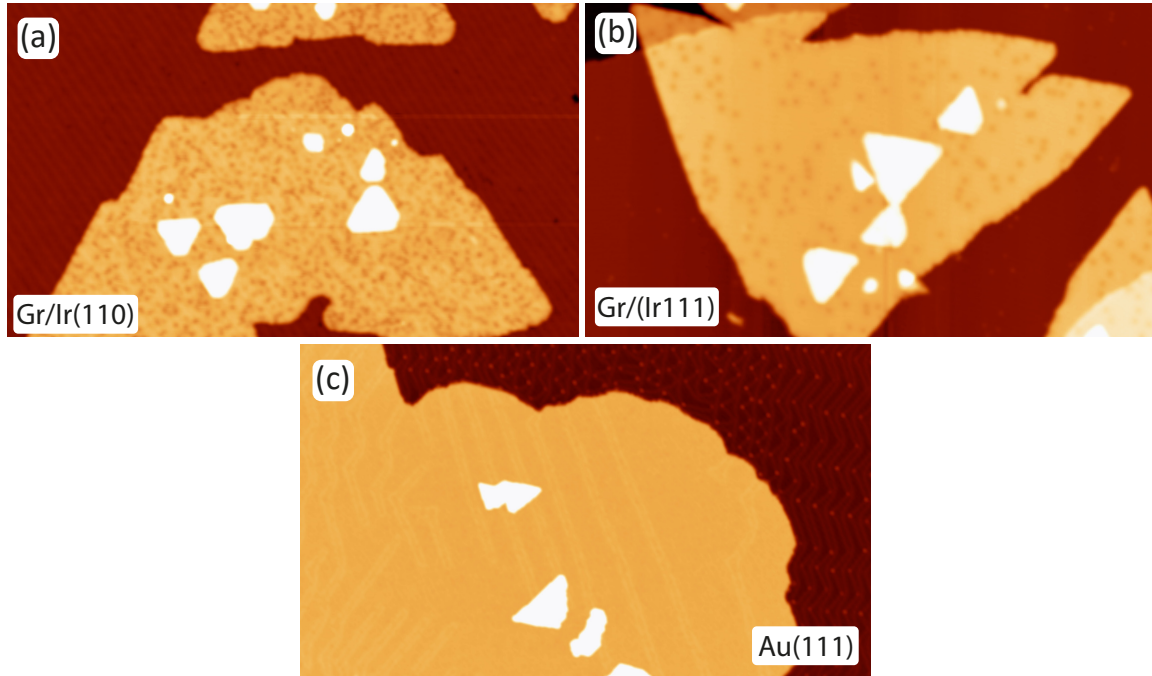


Figure S3. (a) Overview STM topographs of MnBr₂ on (a) Gr/Ir(110), (b) Gr/Ir(111) and (c) Au (111). STM Imaging Parameters: (a) $V_b = 3.5$ V, $I_t = 20$ pA, (b) $V_b = 3.5$ V, $I_t = 20$ pA, (c) $V_b = 2$ V, $I_t = 50$ pA. Image sizes: 240 nm \times 140 nm.

On top of single-layer MnBr₂ islands also small second-layer MnBr₂ islands are visible. The overview STM image of MnBr₂ on Au(111) in Figure S3 shows the herringbone reconstruction in the island, which is only partly lifted by MnBr₂ overgrowth.

Supplementary note 4: Polaron in MnBr_2 on Gr/Ir(111)

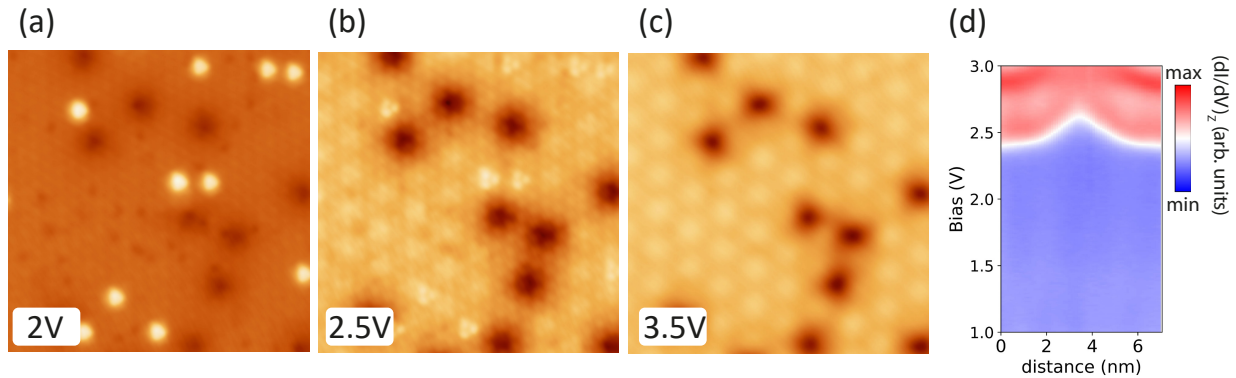


Figure S4. (a-c) Consecutive STM topographs of MnBr_2 on Gr/Ir(111) at different V_b as indicated. (d) Constant current dI/dV linescan map over the type-I immobile. Spectra are acquired with $V_{st} = +3$ V, $I_{st} = 50$ pA, $f_{mod} = 667$ Hz, and $V_{mod} = 20$ mV. STM imaging parameters: $I_t = 50$ pA. Image sizes: 18 nm \times 18 nm.

Supplementary note 5: Tip induced conversions of type-II 1x1 polarons into type-I mobile polarons.

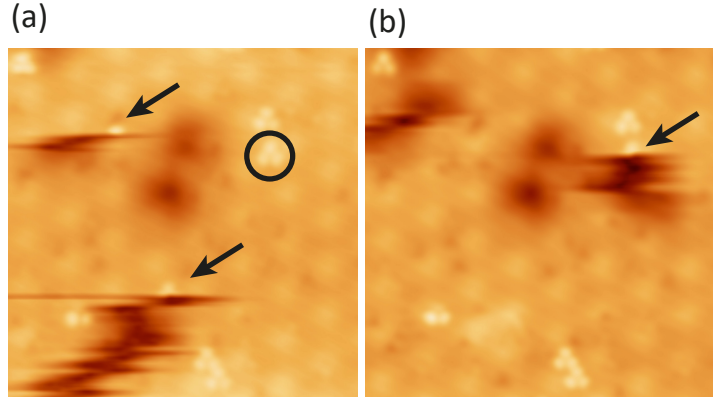


Figure S5. (a,b) Consecutive STM topographs of MnBr_2 on $\text{Gr}/\text{Ir}(111)$. The black arrows in (a) indicate locations where the STM tip induces a conversion from a type-II 1x1 polaron to type-I mobile polaron. Additionally, also the type-II 1x1 polaron circled in (a) has converted to a type I mobile polaron in (b), as highlighted by the arrow in (b). STM imaging parameters: $V_b = 2.5 \text{ V}$, $I_t = 50 \text{ pA}$. Image sizes: $18 \text{ nm} \times 18 \text{ nm}$.

Figure S5 demonstrates conversions of type-II 1x1 polarons to type-I mobile polarons induced during STM scanning. After these conversions, the type-I mobile polarons move with the tip, appearing as fuzzy and continuous dark features in the topographs.

Supplementary note 6: Creation of a type-I 1x1 mobile polaron in MnBr_2 on Gr/Ir(111).

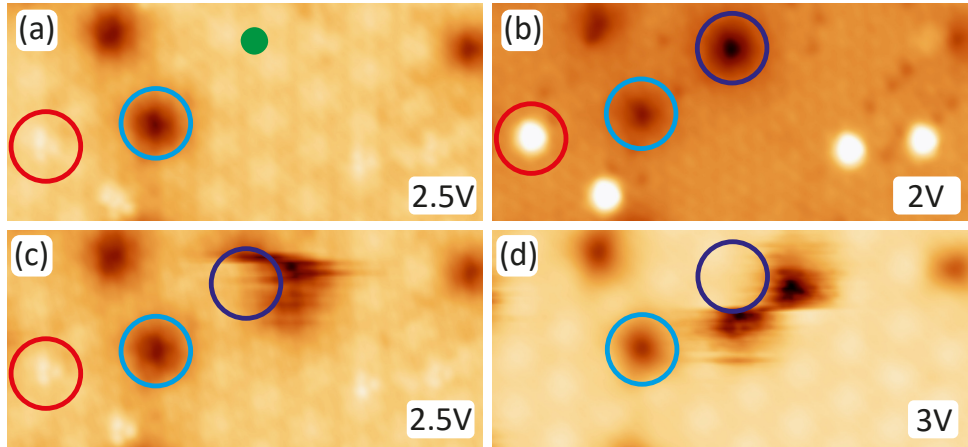


Figure S6. Sequence of STM images illustrating the creation of a type-I mobile polaron in MnBr_2 on Gr/Ir(111) via bias pulsing. (a) STM topograph before bias pulsing with pre-existing type-II 1x1 and type-I immobile polarons (circled red and light blue, respectively). (b) STM topograph after bias pulse with $V_b = +3.5$ V and $I_t = 500$ pA at green dot in (a). (c,d) Subsequent imaging at higher biases shows the mobile polaron moving under the influence of the STM tip. $I_t = 50$ pA. Image sizes: 22 nm \times 10 nm.

Figure S6 shows the creation of a type-I mobile polaron. A bias pulse ($V_b = +3.5$ V, $I_t = 500$ pA) is applied at the green spot in Figure S6 (a). Subsequent imaging at $V_b = +2$ V, as shown in Figure S6(b), reveals a type-I mobile polaron (encircled purple) at pulse location along with pre-existing type-I immobile (encircled blue) and type-II 1x1 polarons (encircled red). In subsequent imaging at $V_b = +2.5$ V and +3 V in Figure S6(c) and (d) the observed mobility of the polaron justifies its classification as type-I mobile polaron.

Supplementary note 7: Bias dependent absolute tip heights above Gr/Ir(110) and MnBr₂/Gr/Ir(110).

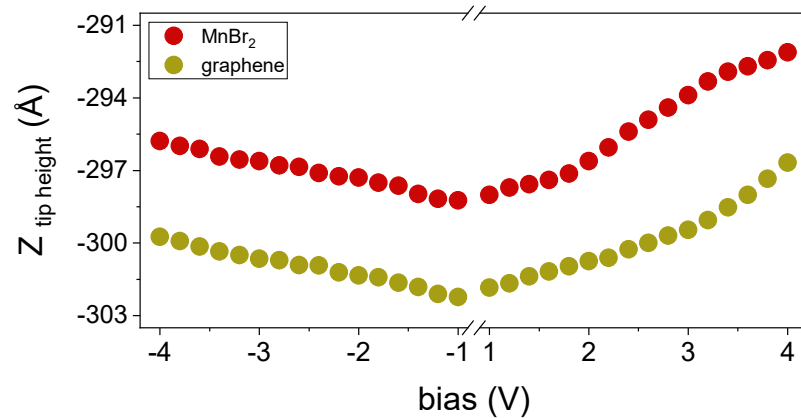


Figure S7. Absolute heights of the STM tip over Gr/Ir(110) (red squares, right y -axis) and MnBr₂/Gr/Ir(110) (black squares, left y -axis) for $I_t = 20$ pA as a function of V_b .